Eur. Phys. J. C 29, 587–595 (2003)
Digital Object Identifier (DOI) 10.1140/epjc/s2003-01249-6

THE EUROPEAN PHYSICAL JOURNAL C

Precision measurements of Higgs–chargino couplings in chargino pair production at a muon collider

H. Fraas[1], F. Franke[1], G. Moortgat-Pick[2], F. von der Pahlen[1], A. Wagner[1]

[1] Institut für Theoretische Physik, Universität Würzburg, Am Hubland, 97074 Würzburg, Germany
[2] Institute for Particle Physics and Phenomenology, University of Durham, Durham DH1 3LE, UK

Received: 6 March 2003 / Revised version: 21 May 2003 /
Published online: 3 July 2003 – © Springer-Verlag / Società Italiana di Fisica 2003

Abstract. We study chargino pair production on the heavy Higgs resonances at a muon collider in the MSSM. At $\sqrt{s} \approx 350\,\mathrm{GeV}$ cross sections up to 2 pb are reached depending on the supersymmetric scenario and the beam energy spread. The resonances of the scalar and pseudoscalar Higgs bosons may be separated for $\tan\beta < 8$. Our aim is to determine the ratio of the chargino couplings to the heavy scalar and pseudoscalar Higgs boson independently of the specific chargino decay characteristics. The precision of the measurement depends on the energy resolution of the muon collider and on the error in the measurement of the cross sections of the non-Higgs channels including an irreducible standard model background. With a high energy resolution the systematic error can be reduced to the order of a few percent.

1 Introduction

Since a muon collider produces Higgs bosons directly via $\mu^+\mu^-$ annihilation in the s-channel, it is an excellent tool to study the properties of a heavy scalar or pseudoscalar Higgs boson [1–4]. Especially the determination of the Higgs couplings constitutes an important test of supersymmetric models. In this paper we explore the potential of a muon collider for a precision measurement of the Higgs–chargino couplings in the minimal supersymmetric standard model (MSSM). Therefore we focus on the chargino pair production in order to determine the chargino couplings to the exchanged Higgs boson in the s-channel.

In the MSSM charginos are the mass eigenstates formed by the mixing of the supersymmetric partners of the charged W and Higgs bosons. While their masses and mixing can be determined with high precision at an e^+e^- collider [5,6], a muon collider is by far the more suitable machine to study their couplings to Higgs bosons. The MSSM contains three neutral Higgs bosons: a light scalar h and two heavier Higgs particles, a scalar H and a pseudoscalar A. Higgs bosons are expected to be discovered at the LHC and studied in the clean environment of a linear e^+e^- collider. However, a linear collider will probably not reveal all properties of the heavy supersymmetric Higgs bosons in detail. The cross sections for the processes $e^+e^- \to Z\{H, A\}$ are heavily suppressed close to the Higgs decoupling limit [7]. The main production mechanism for heavy Higgs bosons is the associated production $e^+e^- \to HA$, which yields cross sections in the fb range [6]. But for a subsequent determination of the Higgs chargino couplings one has to discriminate between charginos from H and A decay. Here it turns out to be rather complicated to find observables which allow one to identify the CP quantum number of the mother particle of the chargino pairs [8]. For beam energies below the HA threshold single Higgs production, $e^+e^- \to H\nu\bar{\nu}$, has been studied in [9]. The small cross section of this process, however, significantly restricts the potential for precision studies of the Higgs properties.

Also the $\gamma\gamma$ mode of a linear collider will not be suitable for a precise measurement of the heavy Higgs bosons to charginos. Although H or A can be resonantly produced, the background from chargino pair production, $\gamma\gamma \to \tilde{\chi}^+\tilde{\chi}^-$, is one order of magnitude larger than the signal $\gamma\gamma \to H, A \to \tilde{\chi}^+\tilde{\chi}^-$ [10]. Furthermore one has to deal with a significantly larger energy spread compared to a muon collider.

A muon collider could overcome these difficulties by providing a heavy Higgs factory [1,2]. In a relevant part of the parameter space the Higgs branching ratios for the decay into chargino pairs are sufficient to perform precise measurements of the Higgs–chargino couplings. In order to be independent of the specific chargino decay mechanism we focus on the ratio of the chargino couplings to the scalar and pseudoscalar Higgs. Then the relevant observables are merely the total cross sections at the H and A resonances and the contribution of the non-Higgs channels that can be measured without any model-dependent assumptions.

The achievable precision is generally limited by the energy resolution of the muon collider and the separation of the relevant Higgs channel from the non-resonant contribution in the chargino production process. An es-

sential requirement is that the H and A signals can be clearly separated. Therefore we also study the overlap of the Higgs resonances as a function of the energy resolution and $\tan\beta$.

This paper is organized as follows: In Sect. 2 we give analytical formulae for the cross sections and characterize the observables for the determination of the Higgs–chargino couplings. Section 3 contains numerical results for representative supersymmetric scenarios with different chargino mixing, Higgs masses and values of $\tan\beta$. We show cross sections for the pair production of the light chargino $\mu^+\mu^- \to \tilde{\chi}_1^+\tilde{\chi}_1^-$ and estimate the relative systematic error in the determination of the Higgs–chargino couplings.

2 Analytical formulae

2.1 Lagrangians and cross sections

We study the chargino pair production in the MSSM

$$\mu^+\ \mu^- \to \tilde{\chi}_i^+\ \tilde{\chi}_j^- \tag{1}$$

for CMS-energies $\sqrt{s}$ at the resonances of the heavy neutral Higgs bosons H and A.

This process proceeds via the exchange of H and A in the s-channel, whereas the contribution from the exchange of the gauge bosons γ, Z and of the light Higgs boson h in the s-channel as well as from the t-channel exchange of $\tilde{\nu}_\mu$ constitutes the background in our analysis.

The interaction Lagrangians for chargino production via Higgs exchange are

$$\mathcal{L}_{\mu^+\mu^-\phi} = g\ c^{(\phi\mu)}\bar{\mu}\ \Gamma^{(\phi)}\ \mu\ \phi, \tag{2}$$

$$\mathcal{L}_{\tilde{\chi}^\pm\tilde{\chi}^\pm\phi} = g\ \bar{\tilde{\chi}}_i^+(c_{ij}^{(\phi)\mathrm{L}}P_\mathrm{L} + c_{ij}^{(\phi)\mathrm{R}}P_\mathrm{R})\tilde{\chi}_j^+\phi, \tag{3}$$

with $\phi = H, A, h$, $\Gamma^{(H)} = \Gamma^{(h)} = 1$, $\Gamma^{(A)} = \mathrm{i}\gamma^5$ and implicit summation over i, j.

Explicit expressions for the Higgs–muon couplings $c^{(\phi\mu)}$ can be found in [11]. They are determined by the Higgs mixing angle α and by the ratio of the vacuum expectation values of the two neutral Higgs fields $\tan\beta = v_2/v_1$. The Higgs–chargino couplings $c_{ij}^{(\phi)\mathrm{L}} = c_{ji}^{(\phi)\mathrm{R}*}$ [11] depend on $\tan\beta$, the SU(2) gaugino mass M_2 and the higgsino mass parameter μ that determine the masses and the mixing characters of the charginos.

In the MSSM with CP-conservation the interference between H and A exchange vanishes. Furthermore the interference between the Higgs boson exchange and the γ, Z and $\tilde{\nu}_\mu$ channels is strongly suppressed by a factor $m_\mu/\sqrt{s}$. Therefore the total cross section of the production of chargino pairs $\tilde{\chi}_i^+\tilde{\chi}_j^-$ can be separated into the dominating contributions σ_H^{ij} and σ_A^{ij} from H and A exchange and the background $\sigma_{B,\mathrm{SUSY}}^{ij}$ from γ, Z, $\tilde{\nu}_\mu$ and h exchange,

$$\sigma^{ij} = \sigma_H^{ij} + \sigma_A^{ij} + \sigma_{B,\mathrm{SUSY}}^{ij}. \tag{4}$$

Chargino production via the γ, Z, $\tilde{\nu}_\mu$ channels will have been thoroughly studied at linear colliders [6]. The h exchange contribution can be neglected at the H and A resonances.

At CMS-energy $\sqrt{s}$ the cross sections σ_H^{ij} and σ_A^{ij} are

$$\sigma_\phi^{ij} = \frac{g^2}{4\pi}|c^{(\phi\mu)}|^2 \cdot |c_{ij}^{(\phi)\mathrm{R}}|^2 \cdot B_\phi^{i,j}(s)K_\phi(s), \quad \phi = H, A \tag{5}$$

with

$$K_\phi(s) = \frac{s}{(s-m_\phi^2)^2 + \Gamma_\phi^2 m_\phi^2}, \tag{6}$$

$$B_H^{ij}(s) = \frac{\lambda(s, m_i^2, m_j^2)^{3/2}}{s^3}, \tag{7}$$

$$B_A^{ij}(s) = \frac{\lambda(s, m_i^2, m_j^2)^{1/2}}{s}, \tag{8}$$

$$\lambda(s, m_i^2, m_j^2) = s^2 - 2s(m_i^2 + m_j^2) - (m_i^2 - m_j^2)^2. \tag{9}$$

The total cross section $\sigma^{f_+f_-}$ for the pair production $\mu^+\mu^- \to \tilde{\chi}_i^+\tilde{\chi}_j^-$ with subsequent decays $\tilde{\chi}_i^+ \to f_+$ and $\tilde{\chi}_j^- \to f_-$ factorizes into the production cross section σ^{ij} and the branching ratios for the respective decay channels:

$$\sigma^{f_+f_-}(\sqrt{s}) = \sigma^{ij}(\sqrt{s}) \times \mathrm{BR}(\tilde{\chi}_i^+ \to f_+) \times \mathrm{BR}(\tilde{\chi}_j^- \to f_-). \tag{10}$$

This holds for each of the contributions $\sigma_H^{f_+f_-}$ from H exchange, $\sigma_A^{f_+f_-}$ from A exchange and $\sigma_{B,\mathrm{SUSY}}^{f_+f_-}$ from the background channels in (4).

2.2 Determination of the Higgs–chargino couplings

In the following we consider the pair production of the light chargino $\tilde{\chi}_1^\pm$ that is expected to be among the first kinematically accessible supersymmetric particles at a muon collider. In order to determine the Higgs–chargino couplings one has to separate the Higgs exchange contributions $\sigma_H^{f_+f_-} + \sigma_A^{f_+f_-}$ from the total measured cross sections $\sigma_\mathrm{meas}^{f_+f_-}$, at $\sqrt{s} = m_H$ and $\sqrt{s} = m_A$, respectively. Since the interference between the Higgs channels and the background is negligible we can subtract the contributions $\sigma_{B,\mathrm{SUSY}}^{f_+f_-}$ from the total cross section.

Besides the non-resonant contributions to the chargino pair production one has to consider further background sources from standard model processes. Here W pair production and single W production constitute the main standard model background, which is in principle rather large [6] but can be strongly reduced by appropriate cuts [12]. Then the resonance peaks remain clearly visible above the smooth standard model background $\sigma_{B,\mathrm{SM}}^{f_+f_-}$ which can therefore be included in the subtraction of the non-resonant contribution from the total cross section.

We determine the total background contribution $\sigma_\mathrm{B}^{f_+f_-} = \sigma_{B,\mathrm{SUSY}}^{f_+f_-} + \sigma_{B,\mathrm{SM}}^{f_+f_-}$ by linear interpolation of $\sigma_\mathrm{meas}^{f_+f_-}$ far below and above the resonance energies. The precision of this

Table 1. Reference scenarios with fixed $m_A = 350\,\mathrm{GeV}$, $m_{\tilde{\chi}_1^\pm} = 155\,\mathrm{GeV}$, $\tan\beta = 5$ and $m_{\tilde{\nu}_\mu} = 261.3\,\mathrm{GeV}$. U_{11} and V_{11} (U_{12} and V_{12}) are the gaugino (higgsino) components of the charginos [15]. $c_{11}^{(H)\mathrm{R}}$ and $c_{11}^{(A)\mathrm{R}}$ denote the Higgs–chargino couplings

Scenarios	A	B	C	D	E	F
M_2/GeV	188	217.3	154.9	169.5	400	400
μ/GeV	−188	217.3	−400	400	−154.9	169.5
U_{11}	0.577	−0.632	0.958	−0.943	0.056	−0.184
U_{12}	0.817	0.775	0.288	0.333	0.9984	0.983
V_{11}	0.817	0.775	0.9984	0.983	0.288	0.333
V_{12}	−0.577	−0.632	−0.056	−0.184	−0.958	−0.943
m_H/GeV	352.1	352.3	351.9	352.3	352.2	352.3
Γ_H/GeV	0.67	0.58	0.31	0.32	0.32	0.39
Γ_A/GeV	1.05	1.33	0.43	0.57	0.43	0.64
$c_{11}^{(H)\mathrm{R}}$	0.513	0.347	0.207	0.197	0.207	0.197
$c_{11}^{(A)\mathrm{R}}$	0.417	0.472	0.192	0.251	0.192	0.251

estimate obviously depends on the variation of the background contributions around the heavy Higgs resonances. By this procedure we avoid, however, reference to other experiments at different energy scales as e.g. chargino production at e^+e^- colliders combined with specific model calculations.

Due to their factorization into production and decay, the ratio of the measured contribution from H and A exchange

$$r = \frac{\sigma_{\mathrm{meas}}^{f_+f_-}(m_H) - \sigma_{\mathrm{B}}^{f_+f_-}(m_H)}{\sigma_{\mathrm{meas}}^{f_+f_-}(m_A) - \sigma_{\mathrm{B}}^{f_+f_-}(m_A)} = \frac{\sigma_H^{11}(m_H) + \sigma_A^{11}(m_H)}{\sigma_H^{11}(m_A) + \sigma_A^{11}(m_A)} \tag{11}$$

is independent of the specific chargino decay channel which may be chosen to give the best experimental signal. Then the measurement of the total cross section for chargino production and decay at the Higgs resonances offers an interesting possibility to determine the ratio of the Higgs–chargino couplings

$$x = \left(\frac{c_{11}^{(H)\mathrm{R}}}{c_{11}^{(A)\mathrm{R}}}\right)^2. \tag{12}$$

From (5) and (11) one obtains

$$x = \frac{r}{C} \cdot \frac{1 - C_1/r}{1 - C_2/r} \cdot \frac{1}{x_\mu}, \tag{13}$$

with

$$C = \frac{\beta^3(m_H^2)}{\beta(m_A^2)} \frac{\Gamma_A^2}{\Gamma_H^2}, \tag{14}$$

$$C_1 = \frac{\beta(m_H^2)}{\beta(m_A^2)} K_A(m_H^2) \Gamma_A^2, \tag{15}$$

$$C_2 = \left(\frac{\beta(m_A^2)}{\beta(m_H^2)}\right)^3 K_H(m_A^2) \Gamma_H^2, \tag{16}$$

$$\beta(s) = \left(\frac{\lambda(s, m_1^2, m_1^2)}{s^2}\right)^{1/4} = \left(\frac{s - 4m_{\tilde{\chi}_1^\pm}^2}{s}\right)^{1/2}, \tag{17}$$

$$x_\mu = \left(\frac{c^{(H\mu)}}{c^{(A\mu)}}\right)^2, \tag{18}$$

where C, C_1 and C_2 can be determined without model-dependent assumptions, and $x_\mu = 1$ in the Higgs decoupling limit.

Assuming that the masses of the heavy Higgs bosons and the chargino are precisely known [6,13] the precision for the determination of x depends on the energy spread of the muon beams, the width of the H and A resonances and on the error in the determination of the background.

3 Numerical results

In the numerical analysis we estimate how precisely the ratio of the couplings of the lighter chargino to the heavy Higgs bosons H and A can be measured. We study the cross sections for the production $\mu^+\mu^- \to \tilde{\chi}_1^+\tilde{\chi}_1^-$ of the lighter chargino with unpolarized beams.

The mass of the scalar Higgs bosons, the widths of A and H and the branching ratios for their decays into charginos are computed with the program HDECAY [14]. The matrix elements of the unitary 2×2 matrices that diagonalize the chargino mass matrix are defined by U_{ij} and V_{ij} [15].

3.1 Scenarios

We choose the six representative scenarios A–F of Table 1 with $m_{\tilde{\chi}_1^\pm} = 155\,\mathrm{GeV}$, $m_A = 350\,\mathrm{GeV}$, and $\tan\beta = 5$

Table 2. Reference scenarios with different mass m_A (scenarios B400 and C400), with different masses $m_{\tilde{\chi}_1^\pm}$ and m_A, (scenarios B180 and C180) and different values of $\tan\beta$ (scenarios B7, B8 and C7, C8) as in the reference scenarios (Table 1). U_{11} and V_{11} (U_{12} and V_{12}) are the gaugino (higgsino) components of the charginos [15]

Scenarios	B400	C400	B180	C180	B7	B8	C7	C8
M_2/GeV	217.3	154.9	242.8	180.7	214	212.8	156.9	157.5
μ/GeV	217.3	−400	242.8	−420	214	212.8	−400	−400
$\tan\beta$	5	5	5	5	7	8	7	8
$m_{\tilde{\chi}_1^\pm}$	155	155	180	180	155	155	155	155
U_{11}	−0.632	0.958	−0.640	0.959	−0.625	−0.622	0.955	0.954
U_{12}	0.775	0.288	0.768	0.283	0.781	0.783	0.297	0.300
V_{11}	0.775	0.9984	0.768	0.9977	0.781	0.783	0.9972	0.9967
V_{12}	−0.632	−0.056	−0.640	−0.068	−0.625	−0.622	−0.075	−0.081
m_A/GeV	400	400	400	400	350	350	350	350
m_H/GeV	402.0	401.6	402.0	401.6	351.2	350.9	351.0	350.7
Γ_H/GeV	1.17	0.61	0.82	0.52	0.71	0.80	0.44	0.53
Γ_A/GeV	2.43	1.09	1.96	1.00	1.42	1.50	0.57	0.67

which differ by the mixing characteristic of the chargino and by the sign of the higgsino mass parameter μ. The parameters, masses and the gaugino and higgsino contents of $\tilde{\chi}_1^\pm$ are given in Table 1. In scenarios A with $\mu < 0$ and B with $\mu > 0$ the light chargino is a wino–higgsino mixing. In scenarios C ($\mu < 0$) and D ($\mu > 0$) it has a dominant gaugino character whereas in scenarios E ($\mu < 0$) and F ($\mu > 0$) it is nearly a pure higgsino.

The additional scenarios in Table 2 are derived from the mixed scenario B and the gaugino scenario C by varying $\tan\beta$ and the masses of the light chargino and the pseudoscalar Higgs boson.

In order to study the influence of the Higgs mass, m_A is increased from $m_A = 350\,\text{GeV}$ to $m_A = 400\,\text{GeV}$ in scenarios B400 and C400. The influence of the chargino mass will be analyzed with the help of scenarios B180 and C180 where $m_{\tilde{\chi}_1^\pm} = 180\,\text{GeV}$ and $m_A = 400\,\text{GeV}$ in order to ensure $m_A > m_{\tilde{\chi}_1^\pm}/2$. However, the character of the light chargino is nearly identical in scenarios B, B180 and B400 (gaugino–higgsino mixing) and in scenarios C, C180 and C400 (gaugino-like), respectively.

Finally we study the influence of the higher values of $\tan\beta = 7$ and $\tan\beta = 8$ for $m_A = 350\,\text{GeV}$ and $m_{\tilde{\chi}_1^\pm} = 155\,\text{GeV}$ in scenarios B7, B8 and C7, C8. To obtain a similar chargino mixing character the parameters M_2 and μ are slightly changed compared to scenarios B and C with $\tan\beta = 5$.

3.2 Branching ratios and cross sections

The branching ratios for the decays of the Higgs bosons H and A into a light chargino pair are crucial for obtaining sufficient cross sections. Therefore we show in Fig. 1 contour plots for the branching ratios in the M_2–μ plane for $\tan\beta = 5$ and $m_A = 350\,\text{GeV}$ and indicate our scenarios A–F.

Since the Higgs bosons couple to both the gaugino and higgsino component of the chargino, the couplings and branching ratios are large in the parameter region $|M_2| \approx |\mu|$ of the mixed scenarios A and B. In scenario A (B) with $\mu < 0$ ($\mu > 0$) one obtains branching ratios up to 45% (20%) for the A decay and up to 20% (15%) for the H decay. In scenarios C and D with a gaugino dominated light chargino as well as in scenarios E and F with a higgsino-like light chargino branching ratios between 20% and 30% for the A decay and between 10% and 20% for the H decay can be observed.

The production cross sections σ^{11} ((4)) for the scenarios A–F are shown in Fig. 2a–f. The heights of the Higgs resonances depend both on their total widths and on the Higgs–chargino couplings (cf. (5) and (6))

$$\sigma_\phi^{11} \propto |c_{11}^{(\phi)\mathrm{R}}|^2/\Gamma_\phi^2, \quad \phi = H, A. \tag{19}$$

The interplay of these parameters (see Table 1) can be observed in Fig. 2. In our scenarios the pattern of the A resonance is determined by the width, whereas for the H peaks the influence of the different H–chargino couplings generally predominates. So the A peaks are of equal height in the mixed and gaugino scenarios Fig. 2a,c and larger than in the higgsino scenario Fig. 2e, inversely proportional to the widths. The H resonance is largest in the scenario with the largest Higgs–chargino coupling Fig. 2a. Only comparing Fig. 2e,f the relative height of the H peak is determined by their width since the couplings are equal due to an approximate symmetry under $|\mu| \leftrightarrow M_2$.

Essential requirements for a precise determination of the Higgs–chargino couplings are distinct resonance peaks and a clear separation of the Higgs resonances. Near threshold the A resonance peak is suppressed by a factor β, compared to a suppression by β^3 of the H resonance. This effect explains the relative height of the resonances in Fig. 2.

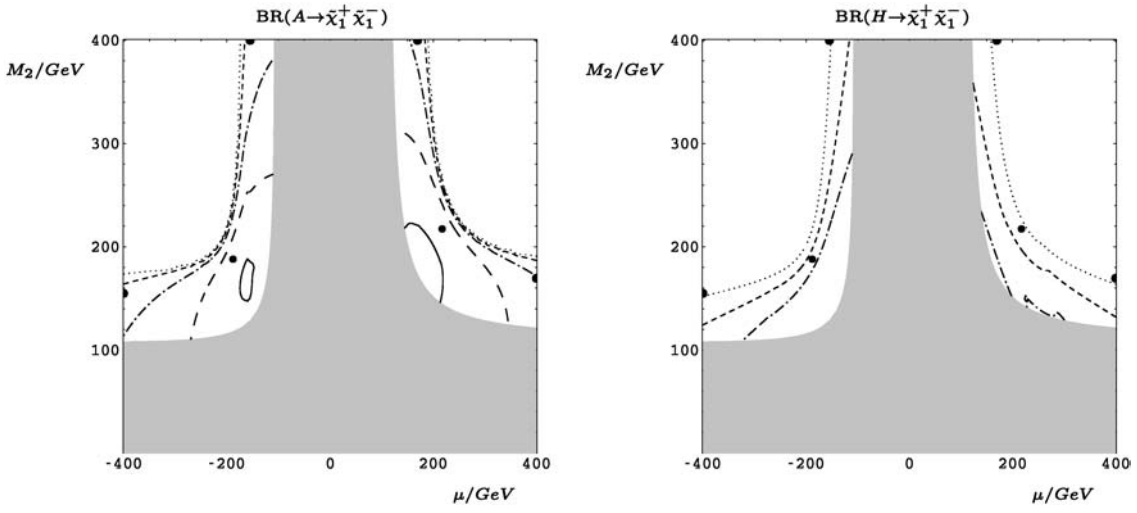

Fig. 1a,b. Branching ratios of the heavy Higgs bosons A and H into light chargino pairs for $m_A = 350\,\text{GeV}$, $\tan\beta = 5$ and sfermions masses larger than $M_H/2$, computed with the program HDECAY [14]. The contour lines correspond to 0.1 (dotted), 0.2 (dashed), 0.3 (dash-dotted), 0.4 (large dashed) and 0.5 (solid). The gray area is the experimentally excluded region given here by $m_{\tilde{\chi}_1^\pm} < 100$ GeV, the thick dots are the scenarios A–F of Table 1

Whether the resonances can be separated depends on both the Higgs line shape and the energy spread of the muon beams. In Fig. 2a–f we compare the cross sections without and with a Gaussian energy spread of 150 MeV which corresponds to an energy resolution $R \approx 0.06\%$.

The energy spread clearly suppresses the resonance peaks especially in scenarios with gaugino-like and higgsino-like light charginos where the resonances are narrower than in the mixed scenarios. However, also with an energy spread of 150 MeV the H and A resonances are well separated in all scenarios (A–F).

The influence of the Higgs mass m_A and the chargino mass $m_{\tilde{\chi}_1^\pm}$ is illustrated in Fig. 3 for mixed scenarios with $\mu > 0$ and for scenarios with a gaugino-like light chargino and $\mu < 0$. In scenarios B400 and C400 with $m_A = 400\,\text{GeV}$ and $m_{\tilde{\chi}_1^\pm} = 155\,\text{GeV}$ the overlap of the Higgs resonances is larger than in the corresponding scenarios with $m_A = 350\,\text{GeV}$ and the same chargino mass; see Figs. 2b,c. The overlap diminishes when the chargino mass is increased to $m_{\tilde{\chi}_1^\pm} = 180\,\text{GeV}$ in scenarios B180 and C180 due to the smaller phase space of the Higgs decays.

For larger values of $\tan\beta$ the A and H resonances tend to overlap since the mass difference diminishes. As an example we compare in Fig. 4 for $m_A = 350\,\text{GeV}$ the total cross sections for the gaugino scenarios C, C7 and C8 with $\tan\beta = 5$, $\tan\beta = 7$ and $\tan\beta = 8$ respectively, without and with an energy spread of 150 MeV. Without energy spread both resonances are well separated up to $\tan\beta = 7$ whereas for $\tan\beta = 8$ the H resonance can barely be discerned. With energy spread, however, the overlap for $\tan\beta = 7$ is already so large that the resonances nearly merge. Here the separation of the resonance contributions may not be possible with a good precision. The same conclusion applies to other chargino scenarios, as can be seen for the mixed scenarios B ($\tan\beta = 5$), B7 ($\tan\beta = 7$) and B8 ($\tan\beta = 8$) in Figs. 4c,d without and with energy spread of 150 MeV, respectively.

4 Precision measurements of the Higgs–chargino couplings

The error in the determination of the ratio x of the squared Higgs–chargino couplings (12) depends both on the energy resolution R of the muon beams and on the error $\Delta\sigma_\text{B}/\sigma_\text{B}$ in the measurement of the non-resonant channels (γ, Z, $\tilde{\nu}_\mu$ and h exchange as well as irreducible standard model background) at the H and A resonances. This background contribution can be estimated from cross section measurements sufficiently far off the Higgs resonances.

In Fig. 5 we plot contours of the relative error in the determination of x in the R and $\Delta\sigma_\text{B}/\sigma_\text{B}$ plane for the scenarios A–F. The contours are shown for the two cases that the irreducible standard model background is neglected or reduced to 25% of the non-resonant supersymmetric channels by appropriate cuts, respectively. For a detailed background analysis Monte Carlo simulations taking into account the detailed detector characteristics have to be performed and are expected to correspond to the considered range in Fig. 5 [12].

As a result of the error propagation one observes a stronger dependence on R than on $\Delta\sigma_\text{B}/\sigma_\text{B}$. Since the energy spread only changes the shape of the resonance the relative errors in the peak cross sections and in the widths are correlated. Generally, an irreducible standard model background up to 25% of the supersymmetric background leads to a slightly reduced precision for the determination of x.

Due to the narrower resonance widths the energy resolution R affects the relative error in x in scenarios C, D and E, F with gaugino-like or higgsino-like light charginos sig-

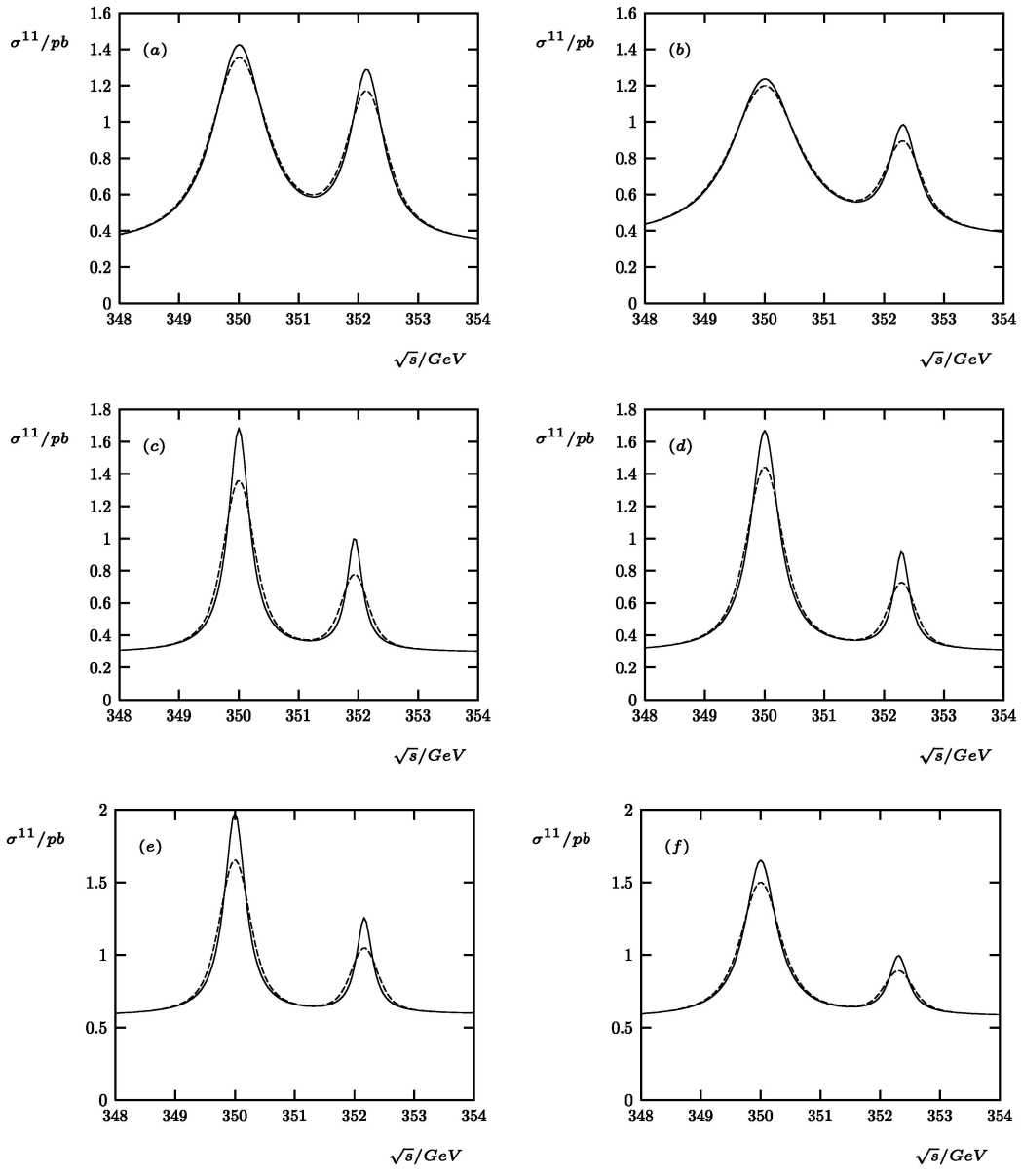

Fig. 2a–f. Total cross section σ^{11} for $\mu^+\mu^- \to \tilde{\chi}_1^+\tilde{\chi}_1^-$ in mixed, gaugino and higgsino scenarios with $\mu < 0$ ($\mu > 0$), **a** (**b**), **c** (**d**) and **e** (**f**) respectively, corresponding to the scenarios A (B), C (D) and E (F) of Table 1. In all scenarios $\tan\beta = 5$, $M_A = 350\,\mathrm{GeV}$, $m_{\tilde{\chi}_1^+} = 155\,\mathrm{GeV}$ and $m_{\tilde{\nu}_\mu} = 261\,\mathrm{GeV}$. The dashed line corresponds to an energy spread of 150 MeV, the solid line to no energy spread

nificantly more than in the mixed scenarios A and B. The influence of the error in the background measurement is largest in the scenarios with a higgsino-like light chargino and much smaller in the other chargino mixing scenarios. In all cases only minor differences appear between the scenarios with positive and negative μ.

In order to achieve a relative error $\Delta x/x < 10\%$ an energy resolution $R < 0.04\%$ is necessary in the mixed scenarios and less than 0.02% in the gaugino and higgsino scenarios. These values lie in the range between 0.01% and 0.06% of the expected energy resolution at a muon collider [3,4]. In addition, the background contributions have to be known with a relative error $\Delta\sigma_\mathrm{B}/\sigma_\mathrm{B} < 10\%$ in the mixed and gaugino scenarios whereas in the higgsino scenarios a much higher precision $\Delta\sigma_\mathrm{B}/\sigma_\mathrm{B} < 6\%$ is necessary.

For an energy resolution of $R = 0.04\%$ the error in the measurement of x becomes $\Delta x/x \approx 40\%$ in scenarios C and D with gaugino-like charginos and practically independent of the background error. A similar error is expected in scenario E with higgsino-like charginos, which decreases to 27% for $\Delta\sigma_\mathrm{B}/\sigma_\mathrm{B} < 10\%$.

If on the other hand an energy resolution $R = 0.01\%$ is achieved and the contributions of the background channels are well known ($\Delta\sigma_\mathrm{B}/\sigma_\mathrm{B} < 5\%$ in the mixed and gaugino scenarios and $\Delta\sigma_\mathrm{B}/\sigma_\mathrm{B} < 2.5\%$ in the higgsino scenarios) the error can be reduced to the order of a few percent.

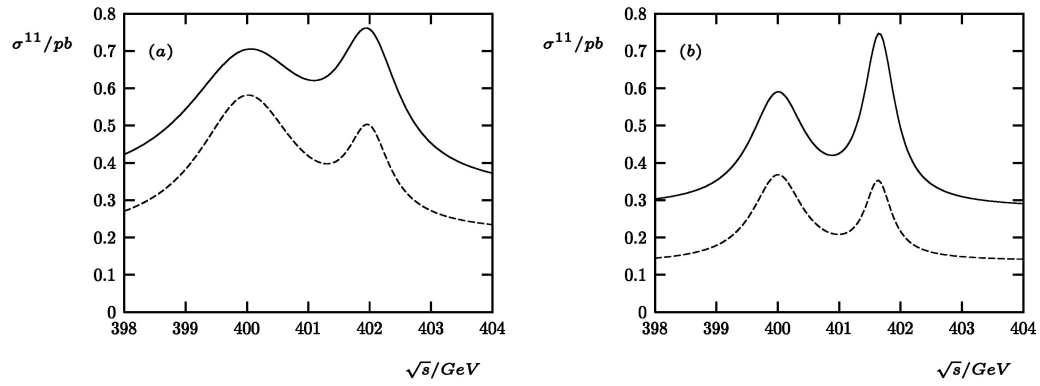

Fig. 3a,b. Total cross section σ^{11} for $\mu^+\mu^- \to \tilde{\chi}_1^+\tilde{\chi}_1^-$ with $\tan\beta = 5$, $M_A = 400\,\text{GeV}$, $m_{\tilde{\nu}_\mu} = 261\,\text{GeV}$ and $m_{\tilde{\chi}_1^+} = 155\,\text{GeV}$ (solid) and $m_{\tilde{\chi}_1^+} = 180\,\text{GeV}$ (dashed). **a** shows the mixed scenarios of Table 2 with $\mu > 0$, B400 and B180, and **b** the gaugino scenarios with $\mu < 0$, C400 and C180, given in Table 2

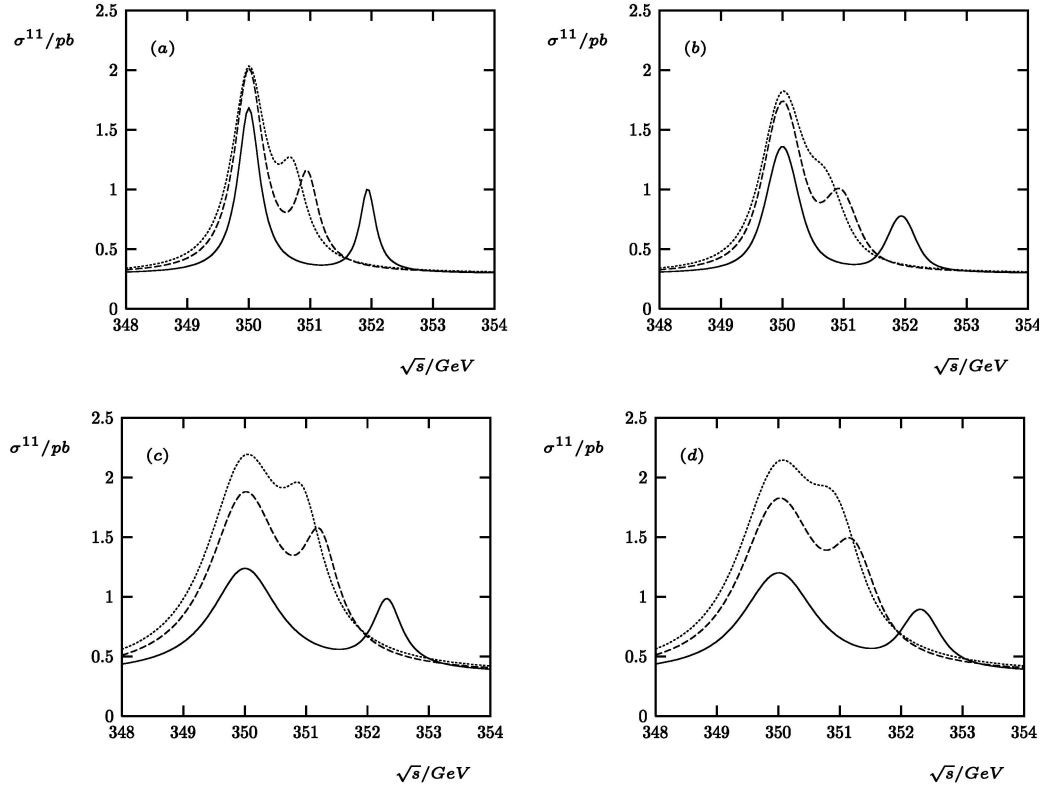

Fig. 4a–d. Dependence on $\tan\beta$ of the total cross section σ^{11} for $\mu^+\mu^- \to \tilde{\chi}_1^+\tilde{\chi}_1^-$ with $M_A = 350\,\text{GeV}$ and $m_{\tilde{\nu}_\mu} = 261\,\text{GeV}$. The gaugino scenarios with $\mu < 0$, C, C7 and C8, are plotted without energy spread **a** and with an energy spread of 150 MeV **b**, for $\tan\beta = 5$ (solid), 7 (dashed) and 8 (dotted), and the mixed scenarios with $\mu > 0$, B, B7 and B8, in **c** and **d**, without and with energy spread respectively and $\tan\beta = 5$ (solid), 7 (dashed) and 8 (dotted)

5 Conclusion

In this paper we have studied chargino pair production at a future muon collider via resonant heavy Higgs boson exchange in the MSSM. This process yields large cross sections of up to a few pb in relevant regions of the supersymmetric parameter space. Due to the sharp energy resolution that allows to separate the CP-even and CP-odd resonances a muon collider is an accurate tool to investigate the Higgs couplings to its decay products. Here we have focused on the determination of the Higgs–chargino couplings. We have shown that the ratio of H-chargino and A-chargino couplings can be precisely determined independently of the chargino decay mechanism. This method avoids reference to other experiments and makes only a few model-dependent assumptions, namely the existence of a CP-even and a CP-odd resonance and the approximate decoupling limit for the Higgs–muon couplings. In representative supersymmetric scenarios we have analyzed the effect of the energy spread and of the error from the

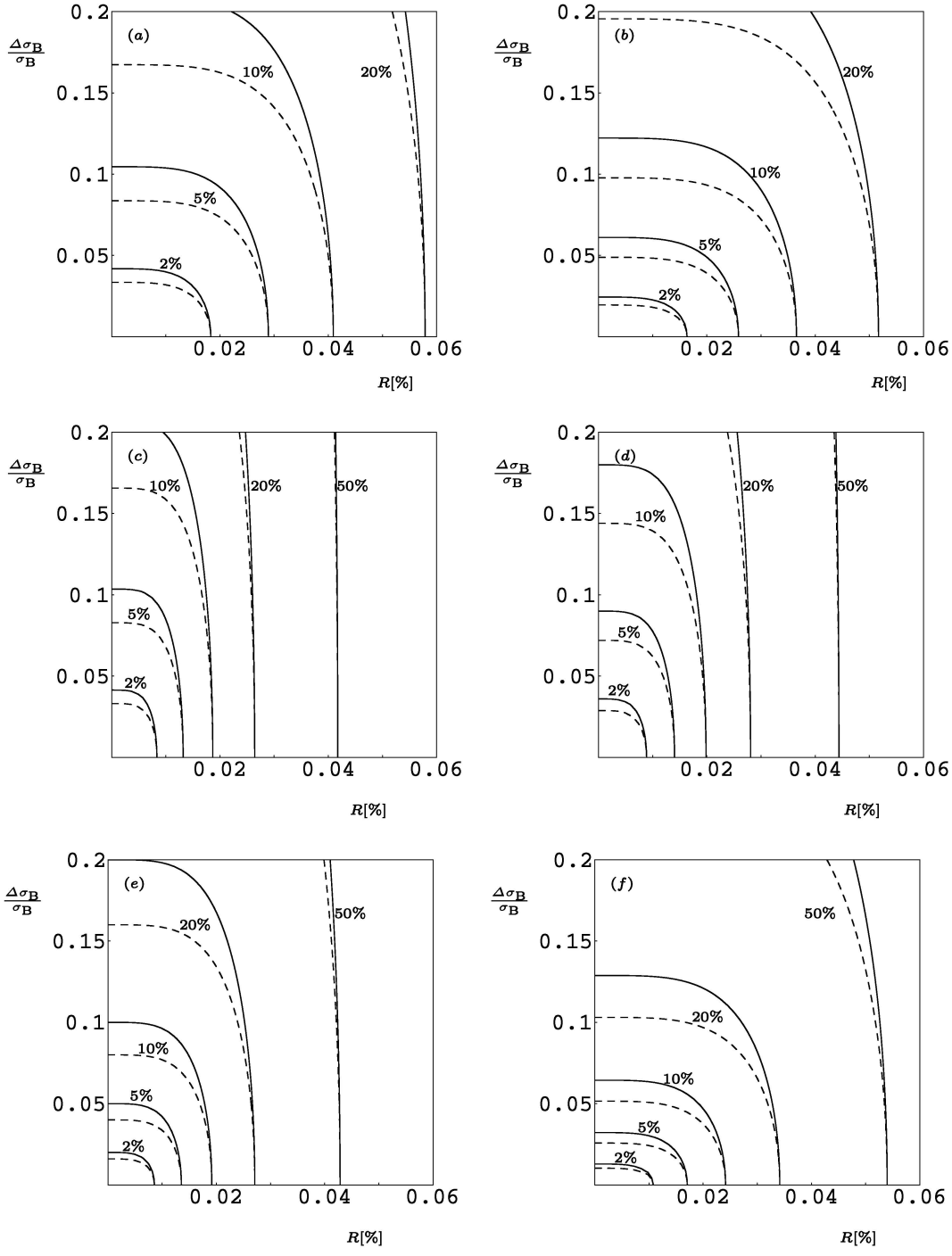

Fig. 5a–f. Relative error in the ratio of the Higgs–chargino couplings x as a function of the energy resolution and the relative error in the non-resonant contributions. The irreducible standard model background is neglected (solid) and 25% of the supersymmetric background (dashed). Plots **a**–**f** correspond to the scenarios A–F in Table 1

non-resonant channels including an irreducible standard model background up to 25% of the supersymmetric background. With a good energy resolution a precision as good as a few percent can be obtained for $\tan\beta < 8$ and $M_A \leq 400\,\mathrm{GeV}$, where the Higgs resonances can be separated.

The precision could be further improved by appropriate beam polarization that enhances the resonant scalar exchange channels and suppresses the background. A loss of luminosity [1,4] as well as effects from initial state radiation and radiative corrections should be taken into account for real simulation studies. The qualitative conclusions of this study, however, remain unchanged.

Acknowledgements. This work was supported by the Bundesministerium für Bildung und Forschung, Contract No. 05 7WZ91P (0), by DFG FR 1064/4-2 and by the EU TMR-Network Contract No. HPRN-CT-2000-00149.

References

1. Proceedings of Prospective Study of Muon Storage Rings at CERN, edited by B. Autin, A. Blondel, J. Ellis, CERN yellow report, CERN 99-02, ECFA 99-197, April 30 (1999)
2. C. Blöchinger et al., Higgs working group of the ECFA-CERN study on Neutrino Factory & Muon Storage Rings at CERN, Physics Opportunities at $\mu^+\mu^-$ Higgs Factories CERN-TH/2002-028, hep-ph/0202199
3. R. Casalbuoni et al., JHEP **9908**, 011 (1999); V. Barger, M.S. Berger, J.F. Gunion, T. Han, in Proceedings of the APS/DPF/DPB Summer Study on The Future of Particle Physics (Snowmass 2001), edited by R. Davidson, C. Quigg, hep-ph/0110340; V. Barger, M.S. Berger, J.F. Gunion, T. Han, Nucl. Phys. Proc. Suppl. A **51**, 13 (1996)
4. V. Barger, M.S. Berger, J.F. Gunion, T. Han, Phys. Rep. **286**, 1 (1997)
5. J.L. Kneur, G. Moultaka, Phys. Rev. D **59**, 015005 (1999); S.Y. Choi, A. Djouadi, M. Guchait, J. Kalinowski, H.S. Song, P.M. Zerwas, Eur. Phys. J. C **14**, 535 (2000); G. Moortgat-Pick, H. Fraas, A. Bartl, W. Majerotto, Eur. Phys. J. C **18**, 379 (2000)
6. TESLA Technical Design Report, DESY 2001-011 Part III: Physics at an e+e- Linear Collider, hep-ph/0106315; ACFA Linear Collider Working Group, KEK Report 2001-11, hep-ph/0109166; T. Abe et al., Linear collider physics resource book for Snowmass 2001. 2: Higgs and supersymmetry studies, in Proceedings of the APS/DPF/DPB Summer Study on the Future of Particle Physics (Snowmass 2001) edited by R. Davidson, C. Quigg, hep-ex/0106056
7. H.E. Haber, Report CERN-TH/95-109, Proceedings Conference on Beyond the Standard Model IV, Lake Tahoe CA 1994, edited by J.F. Gunion et al. (World Scientific) hep-ph/9505240
8. A. Djouadi, J. Kalinowski, P. Ohmann, P.M. Zerwas, Z. Phys. C **74**, 93 (1997)
9. T. Hahn, S. Heinemeyer, G. Weiglein, Nucl. Phys. B **652**, 229 (2003)
10. M.M. Mühlleitner, M. Krämer, M. Spira, P.M. Zerwas, Phys. Lett. B **508**, 311 (2001)
11. J. Gunion, H. Haber, Nucl. Phys. B **272**, 1 (1986)
12. T. Tsukamoto, K. Fujii, H. Murayama, M. Yamaguchi, Y. Okada, Phys. Rev. D **51**, 3153 (1995); A.S. Belyaev, A.V. Gladyshev, hep-ph/9703251
13. V. Barger, M.S. Berger, T. Han, Phys. Rev. D **59**, 071701 (1999)
14. A. Djouadi, J. Kalinowski, M. Spira, Comput. Phys. Commun. **108**, 56 (1998)
15. H. Haber, K. Kane, Phys. Rep. **117**, 75 (1985)